Cytoplasmic mRNA capping enzyme is regulated by hypoxia inducible factor HIF1α and controls stability of the target lncRNAs during hypoxia

Safirul Islam and Chandrama Mukherjee*

Institute of Health Sciences, Presidency University, Plot No. DG/02/02, Premises No. 14-0358, Action Area 1D, Kolkata 700156, India

*Corresponding author, email: chandrama.dbs@presiuniv.ac.in

Email and ORCID IDs for all authors

Safirul Islam: safirul.rs@presiuniv.ac.in, ORCID: 0000-0001-5859-1331

Chandrama Mukherjee: chandrama.dbs@presiuniv.ac.in, ORCID: 0000-0002-4749-1295

Abstract

Hypoxia-inducible factors (HIFs) regulate the expression of several hypoxia-responsive RNAs (HRR) to sustain cellular homeostasis. Cytoplasmic pool of mRNA capping enzyme (cCE) has been shown to recap its substrate uncapped mRNAs or long noncoding RNAs (lncRNAs) present in the cytoplasm, preventing their degradation, even during arsenite-induced oxidative stress. Here, we examined the effect of hypoxia on cCE and its function in regulating the substrate lncRNAs. Hypoxia induces expression of cCE in HIF1α dependent manner as evidenced by Chromatin immunoprecipitation and HIF1α inhibitor experiments. Furthermore, we found cCE post-transcriptionally controls the stability of its target lncRNAs amidst hypoxia. These results suggest that cCE may act as a posttranscriptional modulator that could alter the cellular response to hypoxia by stabilizing cCE-targeted lncRNAs.

Keywords. mRNA capping enzyme/RNGTT, cytoplasmic capping, hypoxia, HIF1α, long noncoding RNA

List of Abbreviations:

CE, mRNA capping enzyme

cCE, cytoplasmic mRNA capping enzyme

HIFs, hypoxia inducible factors

HRR, hypoxia responsive RNA

$CoCl_2$, Cobalt chloride

ChIP, chromatin immunoprecipitation

LncRNA, long noncoding RNA

miRNA, microRNA

circRNA, circular RNA

RNGTT, RNA Guanylyltransferase And 5'-Phosphatase

RNMT, RNA guanine 7-methyl transferase

RAMAC, RNA guanine 7-methyl transferase activating subunit

K294A, dominant negative mutant of cCE

bHLH, basic-helix–loop–helix

LUAD, lung adenocarcinoma

RCC, renal cell carcinoma

Introduction

Hypoxia is one of the contributing factors for generating a solid tumor microenvironment and plays a key role in the progression of tumor metastasis. In 1953 *Gray et. al.* showed the responsiveness of hypoxic tumor cells toward radiotherapy is poor as compared to well-oxygenated tumor cells (1). Additional studies revealed that hypoxia has a profound effect on tumor cell biology which includes its metabolism, angiogenic potential, and sensitivity to chemotherapy or immunotherapy, etc (2). Oxygen-sensitive hypoxia-inducible factor 1α (HIF1α) is the master regulator of hypoxia which reprograms the cellular transcriptomic output in concert with constitutively expressed β subunit so that cells can withstand hypoxic stress (3–5). In addition to HIF1α, several noncoding RNAs like microRNAs (miRNA), long noncoding RNAs (lncRNA), circular RNAs (circRNA)) and epigenetic factors unanimously regulate the cellular response to hypoxia (6).

Cellular stresses are categorized into two groups type 1 and type 2. Hypoxia, heat shock, and arsenite treatment belong to type1 stress whereas genotoxic drugs belong to type2 stress. Cells initiate specific cell stressor mechanisms for their survival upon confronting any environmental stress (7). Studies have indicated that hypoxia markedly reduces *de novo* RNA synthesis mediated by modification of histone acetylation and methylation (8,9). In addition to that cellular response to hypoxia is also achieved at the post-transcriptional level which includes mRNA splicing, stability, etc. Hypoxia-induced transcriptional regulation is well studied whereas its effect on RNA stability at the post-transcriptional level is still not comprehensive. The 5’ cap is one of the crucial factors that determines the stability of an RNA transcript and how this structure is affected during hypoxic stress, remains elusive.

The majority of eukaryotic RNAs that are transcribed by RNA pol II must have a 5’ cap structure which consists of an N^7 methylated guanosine residue that is attached covalently to the first nucleotide of the transcripts by an enzyme called “RNA guanylyltransferase and 5'-phosphatase capping enzyme (RNGTT) or mRNA capping enzyme (CE) ((10,11). Canonical capping takes place inside the nucleus where RNGTT in complex with RNA guanine 7-methyl transferase (RNMT) and RNA guanine 7-methyl transferase activating subunit (RAMAC) act on the 5’end of the nascent RNA transcripts to add a cap (12–14). Later, a pool of cytosolic capping enzymes (cCE) was identified which can recap the uncapped transcripts in the cytoplasm resulting in their stabilization (15,16). cCE forms a complex with the cytoplasmic pool of RNMT, RAMAC along with an unknown 5’RNA kinase and an adaptor protein Nck1 that provides a platform for the assembly of these components to make active cCE that regulates the stability and translability of certain mRNAs and thus has been speculated in maintaining ‘cap homeostasis’ to regulate gene expression (16–18). In agreement with these findings, studies across several labs revealed the presence of uncapped RNAs in various cells pointing to the possibilities of cytoplasmic recapping. Indeed, with the advancement of imaging techniques, mRNAs

have been shown to undergo cyclical decapping and recapping (19). Later, recapping was revealed to act as a nexus of post-transcriptional control as cCE not only regulates mRNAs but also a subset of lncRNAs (20).

Besides these canonical functions of CE/cCE in the protection and maturation of RNA pol II transcribed transcripts or recapping cytosolic transcripts, recent studies have indicated its potential role in various biological processes ranging from modulating the Hedgehog signaling pathway during *Drosophila* development to its involvement in certain cancers (21,22). A current study demonstrates CE governs biliary-derived liver regeneration initiation by transcriptional regulation of mTORC1 and Dnmt1 in Zebrafish (23). Additionally, one recent study uncovers that METTL3 regulates the expression and activity of CE in non-small cell lung cancer (NSCLC) cell lines (24). Recently, a study revealed the role of cCE in protecting the cap status of its target mRNAs during arsenite-induced oxidative stress (25). However, there is no study regarding the effect of hypoxic stress on CE/cCE.

In this study, we examine the effect of hypoxia on the expression of CE or cCE for the first time. Using chemically induced hypoxia on osteosarcoma cell lines (U2OS and MG63) as our model, we found hypoxia elevates the expression of the total pool of CE. Furthermore, we examine the steady state level of previously validated cCE-targeted lncRNAs (20) in hypoxic conditions in cells expressing a dominant negative mutant of cCE (K294A) (20). Our study shows some of these lncRNA are upregulated in hypoxia and cCE regulates their stability indicating its role in post-transcriptional regulation of a subset of hypoxia-responsive lncRNAs.

Materials and methods

Cell culture, treatments, and generation of stable cell lines:

Human osteosarcoma cell line U2OS was purchased from the American Type Culture Collection (ATCC), and MG63 from the National Centre for Cell Science (NCCS, Pune). Both the cell lines were routinely cultured in 1X DMEM (Gibco, cat no# 11965092) supplemented with 10% fetal bovine serum (Himedia, cat no# RM1112) and 1% penicillin-streptomycin (Gibco, cat no# 15140-122) in the presence of 5% CO_2 at 37 □C in a humidified incubator (Eppendorf). Mycoplasma contamination was tested to confirm contamination-free cell culture using a PCR-detection kit (Sigma-Aldrich, cat no# MP0035).

For hypoxia induction *in vitro*, cells were treated with different concentrations (100 µM, 200 µM, and 300 µM) of Cobalt chloride ($CoCl_2$) (Sigma Aldrich, cat no# C8661) solution dissolved in DPBS (Gibco, cat no# 14040182). After 24 hours of treatment, cells were harvested for RNA/protein extraction (26)

HIF1α inhibitor PX478 was procured from the MedChemExpress (cat #HY-10231). 10mM stock of PX478 was prepared by dissolving it in deionized water. Cells were treated with PX478 to a final concentration of 40μM to inhibit HIF1α activity (27).

To generate Control cell line, U2OS cells were transfected with pLenti6/TR vector (kind gift from Dr. Shubhra Majumder, Presidency University), and Blasticidin S Hydrochloride (Sigma Aldrich, cat# 15205) was added to the transfected cells of different dilutions for selection of the clonal cells stably expressing Tetracycline repressor (Tet-R) according to the manufacturer's protocol. Several clones were isolated and examined for the expression of Tet-R protein by western hybridization using an antibody against Tet-R (Novus Biologicals, cat# NB600-234). The clone expressing the highest amount of the repressor was transfected with construct pcDNA4-TO-bio-myc K294A generated in an earlier study (Mukherjee et al, 2024). Zeocin (Invitrogen, cat no# R25001) was added to the cells post 48h transfection at different dilutions. The transfectants were incubated for clonal selection of the stable cells according to the manufacturer's protocols till the isolation of the single colonies. After growing a few selected colonies, Doxycyclin (1ug/ml) (Sigma Aldrich, cat no# D5207) was added to the selected clones for inducible expression of K294A. The stable cell line expressing the highest K294A protein was selected for subsequent experiments.

XTT cell viability assay:

The viability of osteosarcoma cells upon treatment with different concentrations of $CoCl_2$ solution was assessed by using an XTT cell viability assay kit (Cell Signalling Technology, cat no#9095) following the manufacturer's protocol. Briefly, 2000 cells of U2OS/MG63 were seeded in 96 well plates and treated with different concentrations of $CoCl_2$ solutions. 24 hours post-treatment, 50 µl of XTT reagent was added to each well and incubated for 3 h in 5% CO_2 at 37 □C. The absorbance was measured at 450 nm using a BioTek Synergy microplate reader.

Cytoplasmic lysate preparation:

Cells were harvested in ice-cold DPBS and the cell pellet was collected by centrifuging at 1000g for 5 min at 4 □C. Pellet was dissolved in cytoplasmic lysis buffer (20 mM Tris-Cl pH 7.5, 10 mM NaCl,10 mM MgCl2, 10mM KCl, 0.2% NP40, 1 mM PMSF) supplemented with RNaseOUT (Invitrogen, cat no# 10777019) and protease cocktail inhibitor (Roche, cat no# 4693159001). These cell suspensions were kept in ice for 10 minutes with intermittent flicking and then centrifuged at 1000g for 10 min at 4 □C. The supernatant containing cytoplasmic fraction was transferred to a fresh tube.

RNA extraction and poly(A) selection:

Total RNA or cytoplasmic RNA was isolated from cells using TRIzol reagent (Invitrogen cat# 15596026) according to the manufacturer's protocol. RNAs were then treated with DNase I (Thermo Scientific, cat no# EN0521) and extracted using phenol: chloroform: isoamyl alcohol (Sisco Research

Laboratories Pvt Ltd, cat no# 69031). 2µg of DNA-free RNA was used for poly(A) selection using Dynabeads mRNA DIRECT Kit (Invitrogen, cat no# 61011) according to the manufacturer's instruction.

Quantitative real-time PCR analysis:

2 µg of either total RNA or cytoplasmic RNA was reverse transcribed using Super Script III First Strand cDNA Synthesis kit (Invitrogen cat# 18080051) according to the manufacturer's instruction. A 1:1 cDNA dilution was done to perform real-time PCR using SsoAdvanced Universal SYBR Green Supermix (Bio-Rad cat no#172-5271) in CFX connect Real-Time instrument (Bio-Rad). The PCR cycle was carried out using the following thermal conditions initial denaturation at 95 □C for 30 s followed by 40 cycles of 95 □C for 10 s and 60 □C for 15 s and a melting curve was generated by steadily increasing the temperature from 65 □C to 95 □C in 0.5 □C increments with a duration of 2 s/ step. *rplpo* was used as an internal control. The relative fold change of gene expression was calculated using the comparative CT method (ΔΔCt). Unless specified otherwise, at least three different biological replicates were used. The complete list of primers is listed in Table S1.

Western blotting analysis:

Cells were lysed in protein lysis buffer (50 mM Tris-Cl pH 8.0, 150 mM NaCl, and 1% NP-40) supplemented with 1mM PMSF and protease cocktail inhibitor (Roche, cat no# 4693159001). A Rapid Gold BCA Protein Assay kit (Pierce, cat no# A53226) was used to quantify protein samples. 30-60 µg protein extracts were fractionated using 8-10% SDS-PAGE under reducing conditions and transferred onto Immobilon-FL PVDF (Millipore, cat no# IPFL00010) membranes. The membranes were blocked in 3% skimmed milk in phosphate-buffered saline (PBS)for 30 min at room temperature followed by incubation in respective primary antibody dilution. The dilutions are as follows 1:1000 rabbit anti-HIF1α (Cell Signaling Technology, cat no# 36169); 1:1000 mouse anti-beta actin (Santa Cruz Biotechnology, cat no# SC-517582), 1:1000 rabbit anti-CE (Novus Biologicals, cat no# NPB1-49973); 1:2000 mouse anti-GAPDH (Novus Biologicals, cat#2D4A7); 1:2000 rabbit anti-CA9 (Cloud-clone Crop, cat# PAD076Hu01); 1:2000 mouse anti-lamin (DHSB, cat no# MANLAC1(4A7) at 4 □C overnight with constant shaking. Membranes were washed thrice in PBS-T after primary antibody incubation and incubated with secondary antibodies like donkey anti-MouseDyLight 800 (Cell Signaling Technology, cat no#5257) and donkey anti-Rabbit680 (Invitrogen, cat no#A10043) at 1: 10000 dilutions in PBS-T. Blots were scanned in OdysseyCLx Imaging System (LiCor Inc.) and band intensities were calculated using ImageJ software (NIH, USA).

Immunofluorescence:

Cells were cultured on coverslips and fixed in freshly prepared fixing solution [4%PFA(EMS)+0.2% Triton-100 in 1X PBS] for 10 min at room temperature. Coverslips were washed thrice in washing solution (0.5mM $MgCl_2$, 0.05% Triton-100 in 1X PBS) and blocked in blocking buffer (5% FBS,0.2M

glycine, 0.1% Triton-100 in 1X PBS) for 30 min at room temperature. Coverslips were incubated with primary antibodies (1:100, rabbit anti-HIF1α; 1:100 rabbit anti-CE) overnight at 4 □C. Following washing coverslips were incubated with secondary antibodies of donkey IgG conjugated with either Alexa Fluor 488 (Invitrogen cat no# A21206) or 568 (Invitrogen, cat no# A10037) at a dilution of 1:1000 and Hoechst 33358 (Sigma, cat no# 94403) diluted in blocking buffer for 1hr at room temperature. Coverslips were mounted on glass slides with a mounting medium (Invitrogen, cat no# S36967). Images were acquired using a Confocal laser scanning microscope (Leica) fitted with a 63X Plan Apo oil immersion objective (NA 1.4). Images were analyzed, and the fluorescence intensity measurements were performed using the Zeiss Zen 3.3 software package.

Chromatin Immunoprecipitation (ChIP) assay:

HIF1α binding sites on CE promoter were predicted by using JASPAR software (http://www.jaspar.genereg.net). The ChIP assay was performed using a Simple Chip Enzymatic Chromatin IP Kit (Cell Signaling Technology, cat# 9003) as per the manufacturer's instructions. Briefly, the treated/ untreated cells were fixed in 1% formaldehyde for 10 min at room temperature to cross-link the DNA-protein complex. Glycine was added to the cell to quench the unreacted formaldehyde. Following washing with ice-cold PBS containing 1mM PMSF, cells were harvested by centrifugation at 2000 g for 5 min at 4 □C. Cell pellet was lysed in lysis buffer (1× buffer A, 0.5 mM DTT, 1× Protease Inhibitor Cocktail, 1 mM PMSF) and nuclei were pellet down at 2000 g for 5 min at 4 □C. The nuclei pellet was resuspended in buffer B supplemented with 0.5 mM DTT and treated with micrococcal nuclease for 20 min at 37 □C. Following centrifugation at 16000 g for 1 min at 4 □C. Nuclei pellet was resuspended in ChIP buffer (1× ChIP buffer, 1× Protease Inhibitor Cocktail, 1 mM PMSF), followed by sonication to break the nuclei membrane and lysate was clarified by centrifugation at 9400 g for 10 min at 4 □C. 10 µg of chromatin DNA was incubated with rabbit anti-HIF1α (Cell Signaling Technology, cat no# 36169) or normal rabbit IgG (Cell Signaling Technology) overnight at 4°C.To the IP samples protein G magnetic beads were added and incubated 2 hrs at 4°C with rotation. The bead-chromatin-antibody complexes were washed three times in a low-salt wash buffer and one time in a high-salt buffer and eluted in elution buffer heating at 65 °C for 30 min. The proteins were digested by treating them with proteinase K at 65 °C for 2 hrs followed by DNA isolation using a spin column. The immunoprecipitated and input DNA were analyzed by Agarose gel electrophoresis as well as subjected to real-time PCR using SsoAdvanced Universal SYBR Green Supermix (Bio-Rad cat#172-5271) in CFX connect Real-Time instrument (Bio-Rad). The primers for ChIP qPCR are listed in Table S1. Relative fold enrichment was calculated using the comparative CT method (ΔΔCt) described previously where IgG was used as the negative control.

Statistical analysis:

The statistical analysis was calculated by performing Two-tail Student's *t*-tests for two groups and one-way ANOVA for multiple groups using GraphPad Prism 9 Software (GraphPad Software, Inc). All the data were represented as ±SD of at least three independent biological replicates (n=3). Data with $p<0.05$ were considered statistically significant.

Result and Discussion

Hypoxia mimetic $CoCl_2$ augments HIF1α expression in U2OS and MG63 osteosarcoma cells.

The characterization and activity of cCE have been well elucidated in U2OS osteosarcoma cells (15–17,20). Other cell lines like NIH3T3 mouse fibroblasts or human RPE1 (diploid) or primary cells like mouse astrocytes or cardiomyocytes express variable amounts of cCE (25). To determine the effect of hypoxia on the CE/cCE, an *in vitro* chemically induced hypoxic cellular model was established using two osteosarcoma cell lines U2OS and MG63 along with the diploid cell line hTERT RPE-1 (Fig.1, S1). $CoCl_2$ is one of the most commonly used hypoxia mimetic reagents for the induction of chemical hypoxia in cellular models and the presence of HIF1α in the cellular extract is the indicator of successful hypoxia induction (26,28,29). Both U2OS and MG63 cells were exposed to different concentrations (100 µM, 200 µM, and 300 µM) of $CoCl_2$ solution for 24 h and the induction of hypoxia was confirmed by determining the presence of hypoxia marker HIF1α at the protein level by immunoblotting and immunofluorescence staining (Fig. 1). The gradual increase of HIF1α protein expression with the increasing dose of $CoCl_2$ at 24 h was observed in both cell lines (Figs. 1A,1B, 1D, & 1E) which affirms the establishment of hypoxia. Both MG63 and U2OS cells expressed $CoCl_2$ from 100 µM (Figs. 1A and 1D). The toxicity of $CoCl_2$ in the cell lines was examined by performing an XTT cell viability assay (30). Concentration-dependent cytotoxicity of $CoCl_2$ was observed in both cell lines where 300 µM showed the highest toxicity (Figs. 1C and 1F). At 200 µM $CoCl_2$ concentration did not show any toxicity to both the cell lines U2OS and MG63. So, considering the expression of hypoxic marker HIF1α and the minimal cytotoxicity of $CoCl_2$, 200µM was selected for further experiments with both cell lines. The immunofluorescence images of HIF1α also corroborate with the immunoblotting results for induction of hypoxia in U2OS and MG63 cell lines (Figs. 1G and 1H). RPE-1 cells also showed elevated expression of HIF-1α after being treated with 200 µM $CoCl_2$ for 24 h (Figs. S1A and B) suggesting a similar mechanism exists.

$CoCl_2$-induced hypoxia elevates mRNA-capping enzyme expression in osteosarcoma cells

CE protects mRNAs and lncRNAs by adding a 5' cap structure and besides this protection of 5' ends of these RNAs, it also helps the RNA transcripts for their efficient export from the nucleus to the cytoplasm, co-transcriptional processing, and decay (31,32). However, there are a few studies that report the regulation of expression of mammalian CE itself or its recruitment to target genes. A recent study shows catalytically active CE can bind to RNA polymerase II and its target genes in the presence of c-Myc (33). Earlier, we have shown that CE can shuttle between the nucleus and the

cytoplasm and localize to stress granules during arsenite-induced stress (25). However, the impact of other stressors like hypoxia, a major contributing factor to the development of solid tumors on CE is yet to be known. This led us to examine the effect of hypoxia on CE. To understand this, both U2OS and MG63 cells were incubated with $CoCl_2$ for 24 h, followed by staining using CE antibody, and images were captured by a confocal microscope. The immunofluorescence results showed the enhanced expression of total CE in hypoxic conditions as compared to control in both cell lines (Figs: 2A & 2C). We further quantified the mean intensity of CE and our data revealed significant upregulation of CE in hypoxic cells compared with control cells (Figs: 2B & 2D). Later, the mRNA level and protein levels were measured from hypoxic cells and normoxic cells and the results showed increased expression of both RNA and proteins (Fig.4, discussed later). A similar increase in the expression of the total population of CE is also observed in RPE1 cells (Fig. S1C-D). Collectively these data suggest chemical induction of hypoxia increased expression of the total pool of CE in osteosarcoma and human diploid cell lines indicating possible regulation of CE by HIF1α.

Mammalian *rngtt* promoter harbours hypoxia-responsive elements (HRE)

Previous studies showed hypoxia induces the expression of HIF1α (34). Similarly, in our hypoxia model, we observed an accumulation of HIF1α protein during hypoxia (Fig: 1). HIF1α is a member of basic-helix–loop–helix (bHLH)-PAS domain-containing protein family (35) and known to induce the transcription of gene expression by binding to the HRE (R/CGTG) elements present upstream of the transcription start sites in the promoter region (36,37). This led us to speculate that HIF1α might control *rngtt* expression. *In silico* promoter analysis revealed putative HRE sequences in the promoter of *rngtt* as represented schematically in Fig. 3A. The *in-silico* data was validated in hypoxic and normoxic U2OS cells by performing ChIP assay with HIF1α antibody, followed by PCR analysis with different sets of primers targeted to two putative HIF1α binding sites (BS1 & BS2) within 5 kb upstream of the transcription start sites. PCR results showed the direct binding of HIF1α to the *rngtt* promoter in both the binding sites during hypoxia in U2OS cells but not in normoxic conditions (Fig. 3B). The absence of binding of HIF1α may be due to the degradation of HIF1α in the normoxic condition as it is unstable in presence of oxygen (38). Further qPCR analysis revealed that in hypoxic U2OS cells, HIF1α binds to *rngtt* promoter to BS1 and BS2 with 12-fold and 15-fold enrichment respectively, over control IgG (Fig. 3C).

Depletion of HIF1α reduces expression of CE in osteosarcoma cells

To corroborate the ChIP assay results which showed direct binding of HIF1α to *rngtt* promoter, HIF1α was depleted using pharmacological inhibitor PX-478. PX-478 is a well-known inhibitor of HIF-1α (27). It affects its expression both at transcriptional, and translational levels. Moreover, PX-478 prevents de-ubiquitination of ubiquitin-tagged HIF1α molecules (39). Osteosarcoma cells were treated with $CoCl_2$ or kept untreated and PX-478 was added to hypoxia-induced cells. Western blot analysis

showed increased expression of HIF1α in hypoxia-induced samples but decreased expression of HIF1α in PX-478 treated, hypoxia-induced samples in osteosarcoma cells (Figs. 4A-4D). Next, we investigated the effect of HIF1α inhibition on the expression of CE. We observed CE expression also reduced in HIF1α inhibited samples as compared to respective controls in osteosarcoma cells (Figs. 4A-4D). We observed a similar reduction in the level of *rngtt* mRNA in HIF1α inhibited, hypoxic samples compared to control hypoxic samples for both cell lines (Fig. 4E). Therefore, our study showed the elevated expression of CE during hypoxia was due to the direct binding of the HIF1α transcription factor on the rngtt promoter which was abolished upon inhibition of HIF1α.

cCE stabilizes its targeted lncRNAs post-transcriptionally during hypoxia

The hypoxia microenvironment is one of the common features of solid tumors that regulates tumor cells both genotypically and phenotypically (40). Hypoxia, in turn, modulates the expression of various non-coding RNAs to make phenotypic changes in tumor cells, and lncRNAs are one of them (41,42). Previous findings from our group suggested a few lncRNAs could be targeted post-transcriptionally by cCE (20). Considering this fact, we are intrigued to understand whether cCE has any role in regulating its targets during hypoxia. For that, we have chosen ASH1L-AS1, GAS5-215, ENTPD3-AS1, NFYC-AS1, and H19-009 which are related to any of the solid tumors and a few of them established as substrates of cCE (20). H19 and GAS5 lncRNAs are elevated in various tumors (43,44). The other candidate lncRNAs are also involved in developing cancer occurrence and development; such as participation of ASH1L-AS1 in gastric cancer (GC), ENTPD3-AS1 in lung adenocarcinoma (LUAD), and renal cell carcinoma (RCC), NFYC-AS1 in LUAD (45–48).

To analyze the effect of hypoxia on these cCE-targeted lncRNAs, normoxic/hypoxic U2OS cells were separated into nuclear and cytoplasmic fractions efficiently as judged by the detection of Lamin A/C in the nuclear fractions and GAPDH in the cytoplasmic fractions (Fig. 5A). RNA was extracted from cytoplasmic fractions and relative expressions of the candidate lncRNAs were measured using RT-qPCR. We found that out of five lncRNAs, four of them (ASH1L-AS1, GAS5-215, ENTPD3-AS1, and H19-009) were significantly upregulated, whereas the expression of NFYC-AS1 was significantly reduced. As the stability of these lncRNAs was regulated by cCE, we wondered if the upregulated expression of these hypoxia-responsive lncRNAs was contributed by cCE.

To examine this, we made doxycycline-inducible stable U2OS cell lines expressing cytoplasmic restricted, catalytically inactive dominant negative form CE (referred to here as K294A), as schematically represented in Fig 5C. In this cell line, the nuclear localization signal (NLS) was deleted and the nuclear export signal (NES) was added to the CE construct to make it cytoplasm-restricted, as evident from the immunofluorescence image (Fig. 5D). As the control cell line, U2OS cells stably expressing pcDNA6/TR, (Control) was used for subsequent assays. Control and K294A cells were incubated either in normoxic or hypoxic conditions for 24 hrs as described earlier.

Following incubation all the cells were fractionated into nuclear and cytoplasmic fractions. The efficiency of fractions was assessed by western hybridization using antibodies against Lamin A/C and GAPDH as done earlier (Fig. 5E). Our data showed no cross-contamination among the fractions. The expression of CA9, a positive marker for hypoxia, was also checked to confirm the hypoxic condition (Fig. 5E). The steady-state expressions of the candidate lncRNAs in cytoplasmic fractions isolated from Control and K294A cells in normal condition, as well as hypoxic conditions, were measured using RT-qPCR (Fig. 5F & 5G).

In agreement with our previous study (20), no significant changes were observed in the expression of ENTPD3-AS1 during normoxia whereas ASH1L-AS1 showed significant elevation in its expression in K294A-expressing cells (Fig. 5F). However, in contrast to our earlier observation with transiently transfected cells (20), we noticed significantly reduced expressions of GAS5-215, NFYC-AS1, and H19-009 in K294A cells as compared to Control cells under similar conditions (Fig. 5F). This difference may be attributed to the usage of clonal stable cell lines in the current study expressing the similar level of K294A in contrast to a mixed population of cells expressing different levels of K294A along with untransfected cells generated from transient transfection experiments performed in the previous study. Since K294A cells express inactive cCE, the cCE-targeted transcripts like GAS5-215, NFYC-AS1, and H19-009 present in the cytoplasm could not be recapped and would be susceptible to exoribonuclease-mediated degradation resulting in reduced expression in K294A cells (Fig. 5F). On the other hand, ASH1L-AS1 and ENTPD3-AS1 might be protected by some other mechanism that yet to be studied.

Interestingly, we observed the expression of H19-009, which was significantly upregulated in hypoxic control cells, was reduced in hypoxic K294A cells (Fig. 5G). The possible reason could be during hypoxic stress, it might have lost its 5' cap structure and in the absence of active cCE, it could not be recapped, subjected to exoribonucleases. Hence, its expression was reduced in hypoxic K294A cells (Fig. 5G). Furthermore, the expression of GAS5-215 and NFYC-AS1 did not show any significant change in hypoxic K294A cells. We do not have any experimental evidence of how these uncapped transcripts remain stable in hypoxic K294A cells. These data thus suggest that cCE plays an important role in regulating the stability of hypoxic lncRNAs post-transcriptionally.

In this present study, we have examined the effect of hypoxia on the total pool of CE using $CoCl_2$ as a hypoxia mimetic and osteosarcoma cells along with the diploid cell line hTERT RPE-1 as a cellular model. Mechanistically, the enhanced expression of CE/cCE under hypoxia is executed by HIF1α which is a known transcription factor and the master regulator of hypoxia. CE is known to maintain the stability of most RNA pol II transcripts that include both mRNAs and lncRNAs. Besides this, recent studies explore a few of the biological functions of CE in cancer as well as its involvement in the hedgehog signaling pathway. From our study, we observed a global upregulation of CE expression

during hypoxia, however, the significance of this is yet to be investigated. Future research will be conducted on delineating the biological implications of elevated expression CE under hypoxia. As hypoxia is one of the characteristics of solid tumors, so examining the function of CE in this condition would be fruitful for tumor biology research.

Nuclear capping is a co-transcriptional event whereas cytoplasmic capping is a post-transcriptional event. In our previous study, we demonstrated that a subset of lncRNAs is post-transcriptionally stabilized by cCE which recapped the uncapped transcripts present in the cytoplasm. In this study, we examine some tumor-associated lncRNAs and find they are differentially expressed during hypoxia. Importantly, a few of them (H19-009, GAS5-215, and NFYC-AS1) are post-transcriptionally regulated by cCE as evidenced by their decreased expression in K294A cells under normal conditions. Additionally, we observed reduced expression of H19-009 in hypoxic K294A cells which suggests cCE post-transcriptionally regulates the stability of H19-009 during hypoxia as well. However, no significant change in expression was seen for the other two transcripts during hypoxia. Perhaps, the uncapped transcripts are stabilized by some unknown mechanisms like some RNA binding proteins protecting them or they are forming secondary structures where their naked ends are inaccessible to exoribonuclease. Future work will be conducted to decipher how uncapped transcripts remain stable by dissecting their sequences near their uncapped ends and gauging their potential to form stable secondary structures. Further investigation should be carried out to have a comprehensive knowledge of whether all hypoxia-responsive RNAs are substrates of cCE or a few. Taken together our data reveals a novel function of cCE in post-transcriptional regulation of target transcripts during hypoxia.

Acknowledgements

This work was supported by extramural grants CRG/2019/006427 and CRG/2023/006384 from the Department of Science and Technology, Government of India to Dr. Chandrama Mukherjee. The authors also thank UGC, Government of India for a UGC-SRF fellowship to Mr. Safirul Islam and the Department of Biotechnology, India for a Ramlingaswami Re-entry fellowship to Dr. Chandrama Mukherjee. The authors thank the Institute of Health Sciences, Presidency University for the departmental instrument facility and Presidency University for necessary infrastructural support, Dr. Piyali Mukherjee, Presidency University for providing Lamin antibody, Dr. Shubhra Majumder, Presidency University for providing plenti6/TR construct and providing access to Zeiss Microscope and Dr. Abhik Saha, Presidency University for providing access to Licor imager.

Author contributions

SI and CM conceived and designed the experiments. SI performed the experiments described in the study and CM supervised the project. SI and CM wrote different sections of the manuscript. All authors contributed to editing and revising the manuscript, and all authors have approved the final manuscript. The authors have no conflict of interest.

References

1. Gray, L. H., Conger, A. D., Ebert, M., Hornsey, S., & Scott, O. C. (1953). The concentration of oxygen dissolved in tissues at the time of irradiation as a factor in radiotherapy. *The British journal of radiology*, *26*(312), 638–648.
2. Chen, Z., Han, F., Du, Y., Shi, H., & Zhou, W. (2023). Hypoxic microenvironment in cancer: molecular mechanisms and therapeutic interventions. *Signal transduction and targeted therapy*, *8*(1), 70.
3. Parodi, M., Raggi, F., Cangelosi, D., Manzini, C., Balsamo, M., Blengio, F., Eva, A., Varesio, L., Pietra, G., Moretta, L., Mingari, M. C., Vitale, M., & Bosco, M. C. (2018). Hypoxia Modifies the Transcriptome of Human NK Cells, Modulates Their Immunoregulatory Profile, and Influences NK Cell Subset Migration. *Frontiers in immunology*, *9*, 2358.
4. Abou Khouzam, R., Sharda, M., Rao, S. P., Kyerewah-Kersi, S. M., Zeinelabdin, N. A., Mahmood, A. S., Nawafleh, H., Khan, M. S., Venkatesh, G. H., & Chouaib, S. (2023). Chronic hypoxia is associated with transcriptomic reprogramming and increased genomic instability in cancer cells. *Frontiers in cell and developmental biology*, *11*, 1095419.
5. Reheman, A., Wu, Q., Xu, J., He, J., Qi, M., Li, K., Cao, G., & Feng, X. (2024). Transcriptomic analysis of the hypoxia-inducible factor 1α impact on the gene expression profile of chicken fibroblasts under hypoxia. *Poultry science*, *103*(3), 103410.
6. Islam, S., & Mukherjee, C. (2023). Molecular regulation of hypoxia through the lenses of noncoding RNAs and epitranscriptome. *Wiley interdisciplinary reviews. RNA*, *14*(2), e1750.
7. Arimoto, K., Fukuda, H., Imajoh-Ohmi, S., Saito, H., & Takekawa, M. (2008). Formation of stress granules inhibits apoptosis by suppressing stress-responsive MAPK pathways. *Nature cell biology*, *10*(11), 1324–1332.
8. Johnson, A. B., & Barton, M. C. (2007). Hypoxia-induced and stress-specific changes in chromatin structure and function. *Mutation research*, *618*(1-2), 149–162.
9. Johnson, A. B., Denko, N., & Barton, M. C. (2008). Hypoxia induces a novel signature of chromatin modifications and global repression of transcription. *Mutation research*, *640*(1-2), 174–179.
10. Shatkin A. J. (1976). Capping of eucaryotic mRNAs. *Cell*, *9*(4 PT 2), 645–653.
11. Ensinger, M. J., & Moss, B. (1976). Modification of the 5' terminus of mRNA by an RNA (guanine-7-)-methyltransferase from HeLa cells. *The Journal of biological chemistry*, *251*(17), 5283–5291.
12. Ramanathan, A., Robb, G. B., & Chan, S. H. (2016). mRNA capping: biological functions and applications. *Nucleic acids research*, *44*(16), 7511–7526.
13. Pillutla, R. C., Yue, Z., Maldonado, E., & Shatkin, A. J. (1998). Recombinant human mRNA cap methyltransferase binds capping enzyme/RNA polymerase IIo complexes. *The Journal of biological chemistry*, *273*(34), 21443–21446.
14. Varshney, D., Lombardi, O., Schweikert, G., Dunn, S., Suska, O., & Cowling, V. H. (2018). mRNA Cap Methyltransferase, RNMT-RAM, Promotes RNA Pol II-Dependent Transcription. *Cell reports*, *23*(5), 1530–1542.

15. Otsuka, Y., Kedersha, N. L., & Schoenberg, D. R. (2009). Identification of a cytoplasmic complex that adds a cap onto 5'-monophosphate RNA. *Molecular and cellular biology*, *29*(8), 2155–2167.
16. Mukherjee, C., Patil, D. P., Kennedy, B. A., Bakthavachalu, B., Bundschuh, R., & Schoenberg, D. R. (2012). Identification of cytoplasmic capping targets reveals a role for cap homeostasis in translation and mRNA stability. *Cell reports*, *2*(3), 674–684.
17. Mukherjee, C., Bakthavachalu, B., & Schoenberg, D. R. (2014). The cytoplasmic capping complex assembles on adapter protein nck1 bound to the proline-rich C-terminus of Mammalian capping enzyme. *PLoS biology*, *12*(8), e1001933.
18. Trotman, J. B., Giltmier, A. J., Mukherjee, C., & Schoenberg, D. R. (2017). RNA guanine-7 methyltransferase catalyzes the methylation of cytoplasmically recapped RNAs. *Nucleic acids research*, *45*(18), 10726–10739.
19. Iwasaki, S., & Ingolia, N. T. (2016). PROTEIN TRANSLATION. Seeing translation. *Science (New York, N.Y.)*, *352*(6292), 1391–1392.
20. Mukherjee, A., Islam, S., Kieser, R. E., Kiss, D. L., & Mukherjee, C. (2023). Long noncoding RNAs are substrates for cytoplasmic capping enzyme. *FEBS letters*, *597*(7), 947–961.
21. Chen, P., Zhou, Z., Yao, X., Pang, S., Liu, M., Jiang, W., Jiang, J., & Zhang, Q. (2017). Capping Enzyme mRNA-cap/RNGTT Regulates Hedgehog Pathway Activity by Antagonizing Protein Kinase A. *Scientific reports*, *7*(1), 2891.
22. Borden, K., Culjkovic-Kraljacic, B., & Cowling, V. H. (2021). To cap it all off, again: dynamic capping and recapping of coding and non-coding RNAs to control transcript fate and biological activity. *Cell cycle (Georgetown, Tex.)*, *20*(14), 1347–1360
23. Ma, J., Yang, Z., Huang, Z., Li, L., Huang, J., Chen, J., Ni, R., Luo, L., & He, J. (2023). Rngtt governs biliary-derived liver regeneration initiation by transcriptional regulation of mTORC1 and Dnmt1 in zebrafish. *Hepatology (Baltimore, Md.)*, *78*(1), 167–178.
24. Del Valle-Morales, D., Romano, G., Le, P., Saviana, M., Brown, R., Micalo, L., Li, H., La Ferlita, A., Nigita, G., Nana-Sinkam, P., & Acunzo, M. (2023). METTL3 alters capping enzyme expression and its activity on ribosomal proteins. *bioRxiv : the preprint server for biology*, 2023.11.22.568301.
25. Gayen, A., Mukherjee, A., Kumar, K., Majumder, S., Chakrabarti, S., & Mukherjee, C. (2024). The mRNA-capping enzyme localizes to stress granules in the cytoplasm and maintains cap homeostasis of target mRNAs. *Journal of cell science*, *137*(11), jcs261578.
26. Rana, N. K., Singh, P., & Koch, B. (2019). $CoCl_2$ simulated hypoxia induce cell proliferation and alter the expression pattern of hypoxia associated genes involved in angiogenesis and apoptosis. *Biological research*, *52*(1), 12.
27. Tiwari, A., Tashiro, K., Dixit, A., Soni, A., Vogel, K., Hall, B., Shafqat, I., Slaughter, J., Param, N., Le, A., Saunders, E., Paithane, U., Garcia, G., Campos, A. R., Zettervall, J., Carlson, M., Starr, T. K., Marahrens, Y., Deshpande, A. J., Commisso, C., … Bagchi, A. (2020). Loss of HIF1A From Pancreatic Cancer Cells Increases Expression of PPP1R1B and Degradation of p53 to Promote Invasion and Metastasis. *Gastroenterology*, *159*(5), 1882–1897.e5..
28. Muñoz-Sánchez, J., & Chánez-Cárdenas, M. E. (2019). The use of cobalt chloride as a chemical hypoxia model. *Journal of applied toxicology: JAT*, *39*(4), 556–570.
29. Bae, S., Jeong, H. J., Cha, H. J., Kim, K., Choi, Y. M., An, I. S., Koh, H. J., Lim, D. J., Lee, S. J., & An, S. (2012). The hypoxia-mimetic agent cobalt chloride induces cell cycle arrest and alters gene expression in U266 multiple myeloma cells. *International journal of molecular medicine*, *30*(5), 1180–1186.
30. Brosin, A., Wolf, V., Mattheus, A., & Heise, H. (1997). Use of XTT-assay to assess the cytotoxicity of different surfactants and metal salts in human keratinocytes (HaCaT). A feasible method for in vitro testing of skin irritants. *Acta dermato-venereologica*, *77*(1), 26–28.

31. Topisirovic, I., Svitkin, Y. V., Sonenberg, N., & Shatkin, A. J. (2011). Cap and cap-binding proteins in the control of gene expression. *Wiley interdisciplinary reviews. RNA*, *2*(2), 277–298.
32. Schoenberg, D. R., & Maquat, L. E. (2012). Regulation of cytoplasmic mRNA decay. *Nature reviews. Genetics*, *13*(4), 246–259.
33. Lombardi, O., Varshney, D., Phillips, N. M., & Cowling, V. H. (2016). c-Myc deregulation induces mRNA capping enzyme dependency. *Oncotarget*, *7*(50), 82273–82288.
34. Semenza G. L. (2001). HIF-1 and mechanisms of hypoxia sensing. *Current opinion in cell biology*, *13*(2), 167–171.
35. Wang, G. L., Jiang, B. H., Rue, E. A., & Semenza, G. L. (1995). Hypoxia-inducible factor 1 is a basic-helix-loop-helix-PAS heterodimer regulated by cellular O2 tension. *Proceedings of the National Academy of Sciences of the United States of America*, *92*(12), 5510–5514.
36. Semenza, G. L., Agani, F., Booth, G., Forsythe, J., Iyer, N., Jiang, B. H., Leung, S., Roe, R., Wiener, C., & Yu, A. (1997). Structural and functional analysis of hypoxia-inducible factor 1. *Kidney international*, *51*(2), 553–555.
37. Weidemann, A., & Johnson, R. S. (2008). Biology of HIF-1alpha. *Cell death and differentiation*, *15*(4), 621–627.
38. Jaśkiewicz, M., Moszyńska, A., Króliczewski, J., Cabaj, A., Bartoszewska, S., Charzyńska, A., Gebert, M., Dąbrowski, M., Collawn, J. F., & Bartoszewski, R. (2022). The transition from HIF-1 to HIF-2 during prolonged hypoxia results from reactivation of PHDs and HIF1A mRNA instability. *Cellular & molecular biology letters*, *27*(1), 109.
39. Koh, M. Y., Spivak-Kroizman, T., Venturini, S., Welsh, S., Williams, R. R., Kirkpatrick, D. L., & Powis, G. (2008). Molecular mechanisms for the activity of PX-478, an antitumor inhibitor of the hypoxia-inducible factor-1alpha. *Molecular cancer therapeutics*, *7*(1), 90–100.
40. Macharia, L. W., Muriithi, W., Heming, C. P., Nyaga, D. K., Aran, V., Mureithi, M. W., Ferrer, V. P., Pane, A., Filho, P. N., & Moura-Neto, V. (2021). The genotypic and phenotypic impact of hypoxia microenvironment on glioblastoma cell lines. *BMC cancer*, *21*(1), 1248.
41. Barth, D. A., Prinz, F., Teppan, J., Jonas, K., Klec, C., & Pichler, M. (2020). Long-Noncoding RNA (lncRNA) in the Regulation of Hypoxia-Inducible Factor (HIF) in Cancer. *Non-coding RNA*, *6*(3), 27.
42. Peng, P. H., Hsu, K. W., Chieh-Yu Lai, J., & Wu, K. J. (2021). The role of hypoxia-induced long noncoding RNAs (lncRNAs) in tumorigenesis and metastasis. *Biomedical journal*, *44*(5), 521–533.
43. Liu, F. T., Pan, H., Xia, G. F., Qiu, C., & Zhu, Z. M. (2016). Prognostic and clinicopathological significance of long noncoding RNA H19 overexpression in human solid tumors: evidence from a meta-analysis. *Oncotarget*, *7*(50), 83177–83186.
44. Ni W, Yao S, Zhou Y, Liu Y, Huang P, Zhou A, Liu J, Che L, Li J. Long noncoding RNA GAS5 inhibits progression of colorectal cancer by interacting with and triggering YAP phosphorylation and degradation and is negatively regulated by the m^6A reader YTHDF3. Mol Cancer. 2019 Oct 16;18(1):143.
45. Xie, M., Zhang, L., Han, L., Huang, L., Huang, Y., Yang, M., & Zhang, N. (2023). The ASH1L-AS1-ASH1L axis controls NME1-mediated activation of the RAS signaling in gastric cancer. *Oncogene*, *42*(46), 3435–3445.
46. Chiang, H. H., Ong, C. T., Chang, C. Y., Wu, K. L., Wu, Y. Y., Lai, J. C., Shen, T. Y., Hung, J. Y., Lee, H. C., Tsai, Y. M., & Hsu, Y. L. (2024). Downregulated antisense lncRNA *ENTPD3-AS1* contributes to the development of lung adenocarcinoma. *American journal of cancer research*, *14*(2), 854–868.
47. Pandini, C., Pagani, G., Tassinari, M., Vitale, E., Bezzecchi, E., Saadeldin, M. K., Doldi, V., Giannuzzi, G., Mantovani, R., Chiara, M., Ciarrocchi, A., & Gandellini, P. (2024). The pancancer overexpressed NFYC Antisense 1 controls cell cycle mitotic progression through in cis and in trans modes of action. *Cell death & disease*, *15*(3), 206.

48. Song, Y., Du, J., Lu, P., Zou, Q., Zeng, S., Liu, M., Hu, X., Ma, W., Lin, H., Liu, X., & Niu, F. (2021). LncRNA NFYC-AS1 promotes the development of lung adenocarcinomas through autophagy, apoptosis, and MET/c-Myc oncogenic proteins. *Annals of translational medicine*, *9*(21), 1621.

Figure Legends

Figure 1: Hypoxia mimetic $CoCl_2$ augments HIF1α expression in U2OS and MG63 osteosarcoma cells. A & D. Western blot analysis of hypoxic stress marker HIF1α, showing gradual increase upon increasing concentrations of $CoCl_2$ for 24 hrs treatment in U2OS and MG63 osteosarcoma cells respectively. The molecular weight of the proteins is indicated on the left. B & E. Quantification of HIF1α protein by ImageJ software using three independent biological replicates. β-actin was used as the loading control. C & F. XTT cell viability assay showing $CoCl_2$ dose-dependent loss of cellular viability in U2OS and MG63 cells. G & H. Immunostaining analysis showing an elevated expression of HIF1α (green) during hypoxia in osteosarcoma cells. DNA is represented by DAPI. The scale bar represents 50 µm. Values are represented as ± SD from three biological replicates. *ns*, *P*: non-significant, **P*< 0.05, ***P*< 0.005, ****P*< 0.0005, *****P*< 0.0001; n≥3.

Figure 2: $CoCl_2$-induced hypoxia elevates expression of CE/cCE in osteosarcoma cells. A & C. Immunostaining analysis showing enhanced expression of total pool of CE in nucleus or cytoplasm in $CoCl_2$ treated cells as compared to untreated cells. The scale bar represents 50 µm. B & D. Quantification of mean CE intensity using Zeiss Zen 3.3 software package, n≥20 cells. Values are represented as ± SD, *****P*< 0.0001.

Figure 3: The promotor of mammalian CE (rngtt) harbors hypoxia-responsive elements (HRE). A. Human *rngtt* gene contains two HIF1α binding motif (R/CGTG) in its promoter region as shown in the schematic. B. Chromatin immunoprecipitation (ChIP) analysis showed direct binding of HIF1α in the *rngtt* promoter region (BS1 and BS2). 2% input samples were loaded. The molecular weight of the DNA ladder is shown on the left. C. ChIP assay followed by quantitative RT–PCR (qRT–PCR) showed ∼12 and 15-fold enrichment of HIF1α binding to the BS1 and BS2 of *rngtt* promoter region during hypoxia respectively. Values are represented as ± SD from three biological replicates. ns: non-significant, *P< 0.05, **P< 0.005, ***P< 0.0005, ****P< 0.0001; n≥3.

Figure 4: Depletion of HIF1α reduces rngtt expression in osteosarcoma cells. A & C. Western blot analysis shows a significant decrease in the expression of HIFα and CE protein upon treatment with PX-478 in hypoxic conditions. The molecular weight of the proteins is indicated on the left. B & D. Quantification of HIF1α and CE protein by ImageJ software using three independent biological replicates. β-actin was used as the loading control. E. Quantitative RT–PCR (qRT–PCR) analysis revealed treatment of osteosarcoma cells (U2OS and MG63) with 40µM HIF1α inhibitor PX-478 in hypoxic conditions resulting in a significant reduction in *rngtt* expression. Values are represented as ± SD from three biological replicates. ns, P: non-significant, *P< 0.05, **P< 0.005, ***P< 0.0005, ****P< 0.0001; n≥3.

Figure 5: cCE stabilizes its targeted lncRNAs post-transcriptionally during hypoxia. A. Biochemical fractionation of normoxic/hypoxic U2OS cells into nuclear/ cytoplasmic fractions. The quality of fractionation was assessed by immunoblotting of nuclear marker Lamin A/C) and cytoplasmic marker (GAPDH). CA9 immunoblotting was done to confirm the hypoxic condition. B. Realtime PCR of cCE-targeted lncRNAs shows differential expression patterns in cytoplasmic extracts of hypoxic osteosarcoma cells. Hypoxia significantly elevates the expression of ASH1L-AS1,

GAS5-215, ENTPD3-AS1, and H19-009, whereas NFYC-AS1 expression was significantly reduced. Two-tail Student's t-test was performed for statistical analysis C. Schematic representation of the dominant negative form of cytoplasmic restricted capping inhibited construct (K294A) BIO and myc denote the biotinylation and myc tag respectively. The nuclear export sequence (NES) of HIV is inserted in the N-terminus and the Nuclear Localization Signal (NLS) from the C-terminus is deleted to restrict expression of CE only in the cytoplasm. The lysine (K) residue at 294th position is mutated to alanine (A) to make the construct catalytically inactive. D. Immunofluorescence image of myc tagged K294A expressing cells. E. Nuclear and cytoplasmic fractionation of U2OS cells expressing ±K294A under normoxic/hypoxic conditions. Western blot of Myc and CA9 confirm K294A expression and hypoxic condition respectively. The quality of fractionation was further substantiated by western blotting of nuclear marker (Lamin A/C) and cytoplasmic marker (GAPDH). F. The steady-state expression of GAS5-215, NFYC-AS1, and H19-009 was significantly decreased in K294A-expressing cells under normoxia. But ASH1L-AS1 was significantly increased and ENTPD3-AS1 did not show any significant change. G. The steady State expression of lncRNAs in hypoxic K294A cells. Only H19-009 showed significantly reduced expression in hypoxic K294A cells. Statistical significance was calculated by Two-tail Student's t-test. Values are represented as ± SD from three biological replicates. ns, P: non-significant, *P< 0.05, **P< 0.005, ***P< 0.0005, ****P< 0.0001; $n \geq 3$.

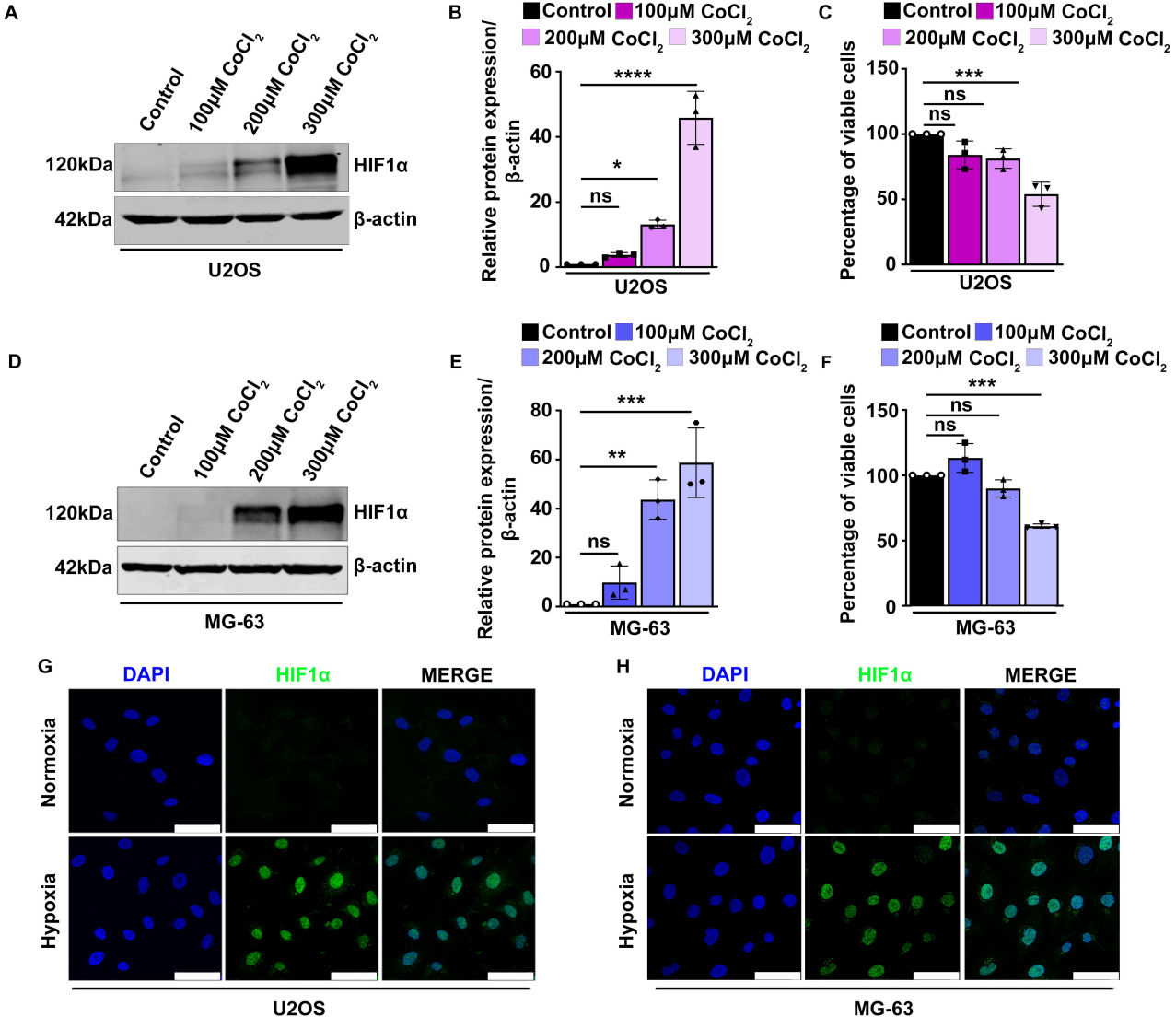
A
Control
100μM CoCl2
200μM CoCl2
300μM CoCl2
120kDa
HIF1α
42kDa
β-actin
U2OS
B
Control
100μM CoCl2
200μM CoCl2
300μM CoCl2
Relative protein expression/ β-actin
****
*
ns
U2OS
C
Percentage of viable cells
***
ns
ns
U2OS
D
MG-63
E
Relative protein expression/ β-actin
***
**
ns
MG-63
F
Percentage of viable cells
***
ns
ns
MG-63
G
DAPI
HIF1α
MERGE
Normoxia
Hypoxia
U2OS
H
MG-63

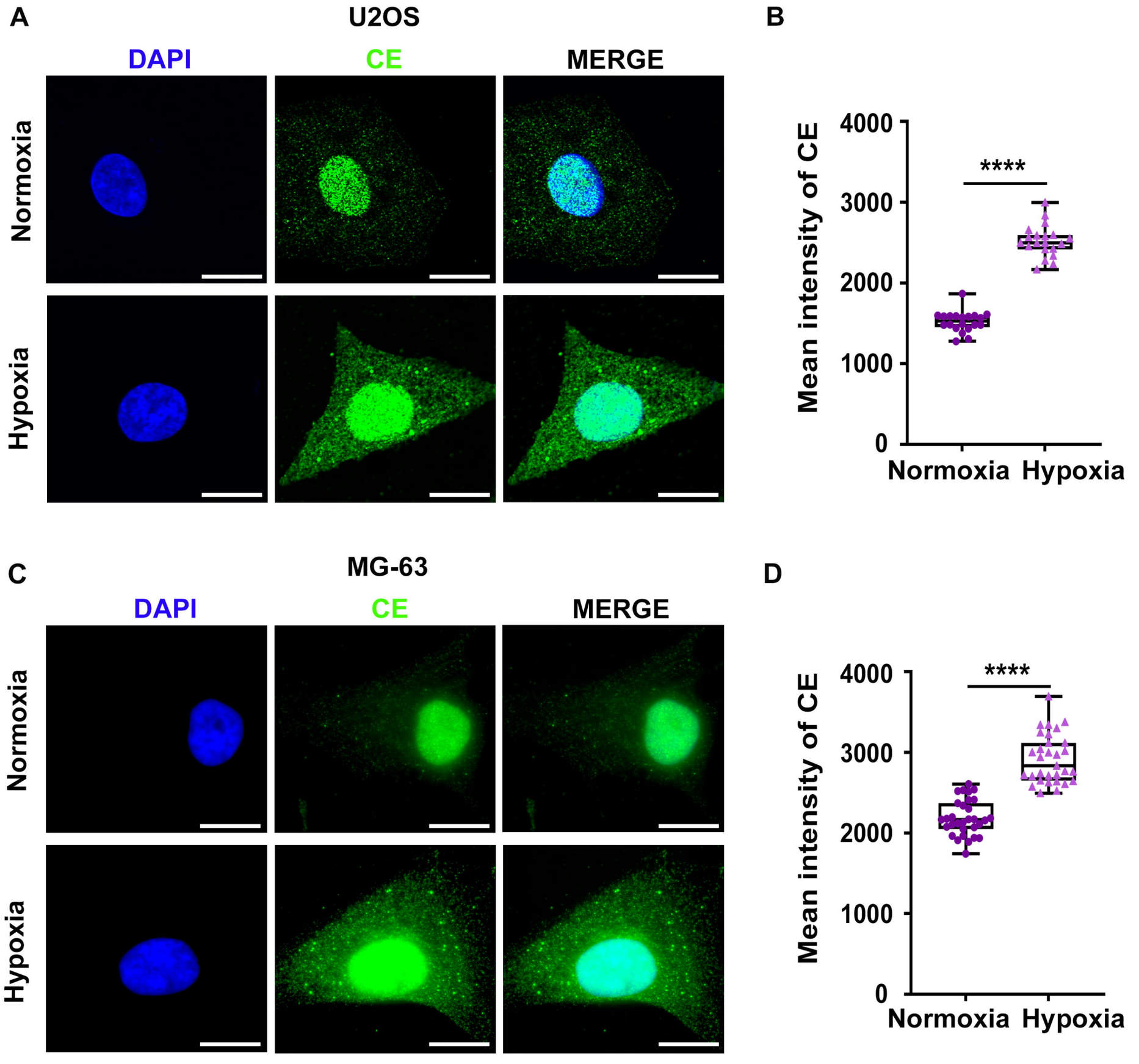
A
U2OS
DAPI
CE
MERGE
Normoxia
Hypoxia
B
Mean intensity of CE
4000
3000
2000
1000
0
****
Normoxia
Hypoxia
C
MG-63
DAPI
CE
MERGE
Normoxia
Hypoxia
D
Mean intensity of CE
4000
3000
2000
1000
0
****
Normoxia
Hypoxia

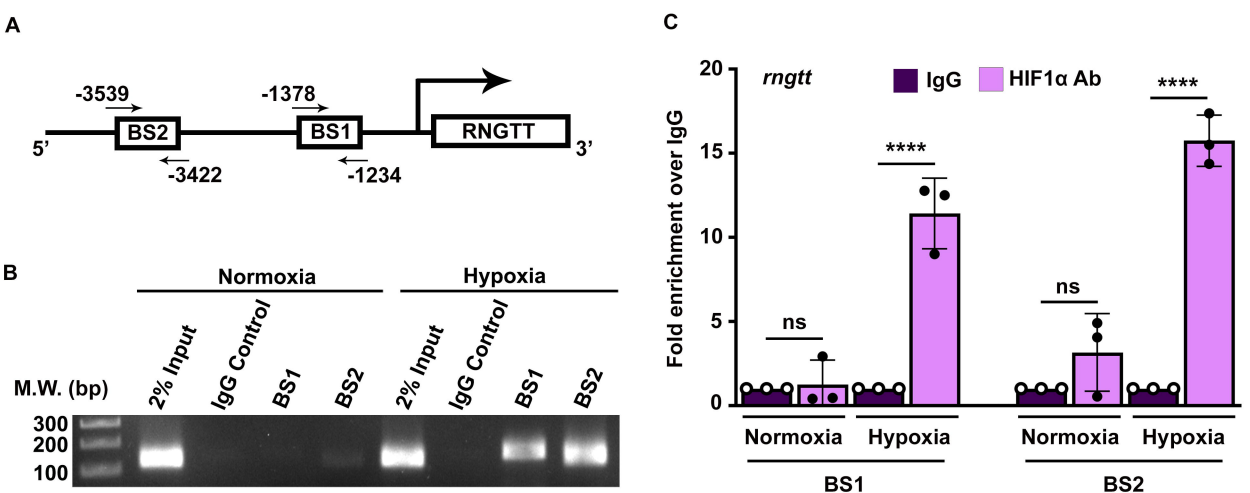
A
-3539
-1378
BS2
BS1
RNGTT
5'
3'
-3422
-1234
B
Normoxia
Hypoxia
M.W. (bp)
2% Input
IgG Control
BS1
BS2
2% Input
IgG Control
BS1
BS2
300
200
100
C
rngtt
IgG
HIF1α Ab
Fold enrichment over IgG
20
15
10
5
0
****
****
ns
ns
Normoxia
Hypoxia
Normoxia
Hypoxia
BS1
BS2

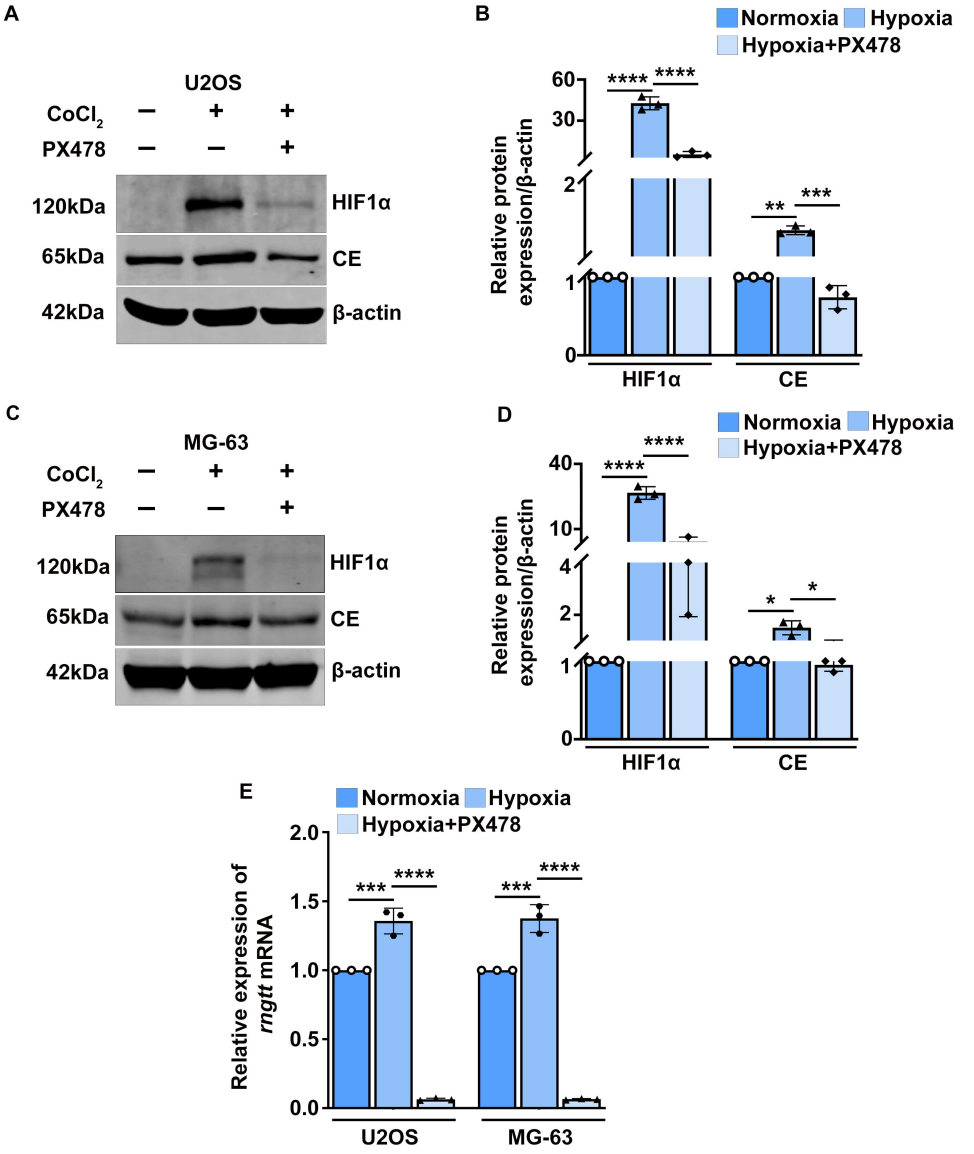
A
U2OS
CoCl2 − + +
PX478 − − +
120kDa
65kDa
42kDa
HIF1α
CE
β-actin
B
Normoxia
Hypoxia
Hypoxia+PX478
Relative protein expression/β-actin
60
30
2
1
0
****
****
**
***
HIF1α
CE
C
MG-63
CoCl2 − + +
PX478 − − +
120kDa
65kDa
42kDa
HIF1α
CE
β-actin
D
Normoxia
Hypoxia
Hypoxia+PX478
Relative protein expression/β-actin
40
10
4
2
1
0
****
****
*
*
HIF1α
CE
E
Normoxia
Hypoxia
Hypoxia+PX478
Relative expression of rngtt mRNA
2.0
1.5
1.0
0.5
0.0
***
****
***
****
U2OS
MG-63

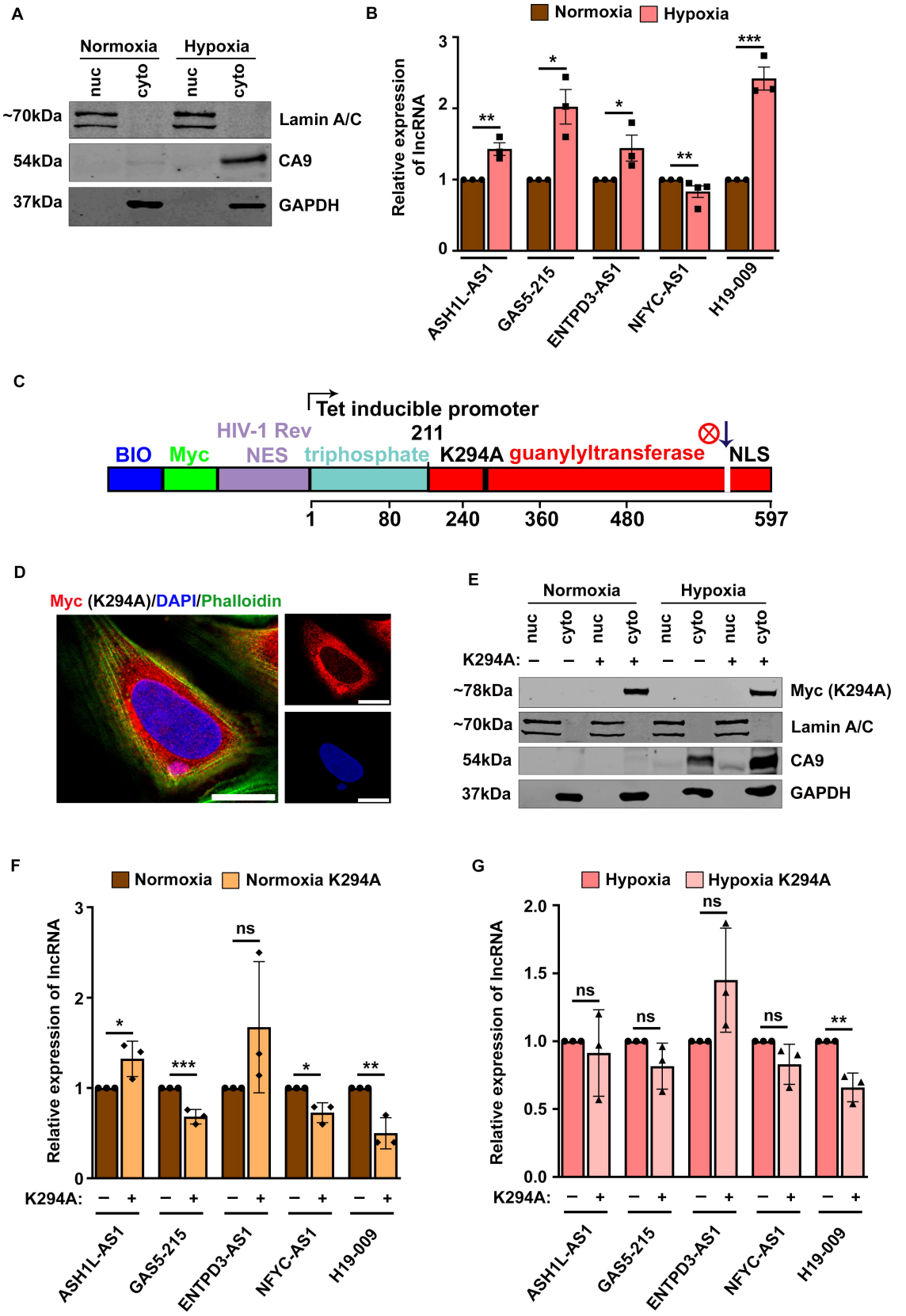
A
Normoxia
Hypoxia
nuc
cyto
nuc
cyto
~70kDa
Lamin A/C
54kDa
CA9
37kDa
GAPDH
B
Normoxia
Hypoxia
Relative expression of lncRNA
ASH1L-AS1
GAS5-215
ENTPD3-AS1
NFYC-AS1
H19-009
C
Tet inducible promoter
HIV-1 Rev
211
BIO
Myc
NES
triphosphate
K294A
guanylyltransferase
NLS
1
80
240
360
480
597
D
Myc (K294A)/DAPI/Phalloidin
E
Normoxia
Hypoxia
nuc
cyto
nuc
cyto
nuc
cyto
nuc
cyto
K294A:
~78kDa
Myc (K294A)
~70kDa
Lamin A/C
54kDa
CA9
37kDa
GAPDH
F
Normoxia
Normoxia K294A
Relative expression of lncRNA
K294A:
ASH1L-AS1
GAS5-215
ENTPD3-AS1
NFYC-AS1
H19-009
G
Hypoxia
Hypoxia K294A
Relative expression of lncRNA
K294A:
ASH1L-AS1
GAS5-215
ENTPD3-AS1
NFYC-AS1
H19-009